Korean Circ J. 2026 Aug;56(8):655-679
https://doi.org/10.4070/kcj.2025.0420
pISSN 1738-5520·eISSN 1738-5555

kcj
Korean Circulation Journal

State of the Art Review

Check for updates

Assessment of Myocardial Stiffness With New Echocardiographic Methods

Laurine Wouters, MSc[1], Annette Caenen, PhD[1,2], Ahmed Youssef, MD[1,3], Andressa Araujo Andrade Sousa, MD[1], Stéphanie Bézy, PhD[1], Jürgen Duchenne, PhD[1,4,5], Jan D'hooge, PhD[1], and Jens-Uwe Voigt, MD, PhD[1,6]

[1]Department of Cardiovascular Sciences, Catholic University Leuven, Leuven, Belgium
[2]Department of Electronics and Information Systems, Ghent University, Ghent, Belgium
[3]Department of Cardiovascular Medicine, Suez Canal University, Ismailia, Egypt
[4]Research Group Cardio & Organ Systems, Hasselt University, Diepenbeek, Belgium
[5]Department of Cardiology, Jessa Hospital, Hasselt, Belgium
[6]Department of Cardiovascular Diseases, University Hospitals Leuven, Leuven, Belgium

OPEN ACCESS

Received: Sep 30, 2025
Revised: Oct 22, 2025
Accepted: Oct 28, 2025
Published online: Dec 2, 2025

Correspondence to
Jens-Uwe Voigt, MD, PhD
Department of Cardiovascular Sciences, Catholic University Leuven, Herestraat 49, Leuven 3000, Belgium.
Email: jens-uwe.voigt@uzleuven.be

ORCID iDs
Laurine Wouters
https://orcid.org/0000-0002-1841-6720
Annette Caenen
https://orcid.org/0000-0002-4747-6482
Ahmed Youssef
https://orcid.org/0000-0002-9014-4432
Andressa Araujo Andrade Sousa
https://orcid.org/0009-0003-7538-8003
Stéphanie Bézy
https://orcid.org/0000-0001-5728-8082
Jürgen Duchenne
https://orcid.org/0000-0003-0221-5753
Jan D'hooge
https://orcid.org/0000-0002-2346-142X
Jens-Uwe Voigt
https://orcid.org/0000-0002-0575-1888

AUTHOR'S SUMMARY

Myocardial stiffness plays a critical role in determining cardiac function, yet its evaluation traditionally relies on invasive procedures. Advances in echocardiography have introduced promising non-invasive approaches. This review highlights the leading ultrasound-based techniques for assessing myocardial stiffness and examines key findings from recent clinical studies in this area.

ABSTRACT

Myocardial stiffness is a key determinant of cardiac function. So far, its assessment required invasive methods such as pressure-volume loop measurements or mechanical testing of tissue biopsies, which are both not suited for daily clinical use. However, recent advances in echocardiography offer promising non-invasive alternatives. Initial clinical studies in different pathologies are encouraging and indicate a huge potential of these new ultrasound-based techniques for evaluating myocardial stiffness. In this review, we explain the concept of myocardial stiffness, explore the most promising ultrasound techniques currently available for its evaluation, and discuss key insights from recent clinical research in the field.

Keywords: Myocardial stiffness; Echocardiography; Shear wave elastography; Time harmonic elastography; Acoustic radiation force imaging

INTRODUCTION

Myocardial stiffness is an important aspect of cardiac function and reflects the intrinsic properties of the myocardium as well as pressure and stress acting on the myocardial wall.[1)2)] Myocardial stiffness is altered in a variety of pathologies so that its correct assessment might help in diagnosis and patient management. Only recently, new imaging-based techniques to evaluate myocardial stiffness became available.[3-7)] In this review, we will focus on echocardiographic techniques, as echocardiography is the most widely used imaging modality in cardiology and adding stiffness assessment to its armamentarium could be

kcj
Korean Circulation Journal

Funding
This work was supported by the Research Foundation Flanders (FWO) under grant 11PP524N to L. Wouters, 12B3124N to dr. A. Caenen, 1832922N to prof. J.-U. Voigt and 12ZZN22N to prof. J. Duchenne. A. Youssef is supported by the European Association of Cardiovascular Imaging (EACVI) research grant (2024 winner), a scholarship from the Egyptian ministry of research and higher education (2021 recipient) and the Belgian Fund for Cardiac surgery (2023–2024). The funders had no role in preparation of the manuscript.

Conflict of Interest
The authors have no financial conflicts of interest.

Data Sharing Statement
The data generated in this study is available from the corresponding author upon reasonable request.

Author Contributions
Resources: Caenen A; Supervision: Caenen A, Youssef A, Duchenne J, D'Hooge J, Voigt JU; Visualization: Araujo Andrade Sousa A, Bézy S; Writing - original draft: Wouters L; Writing - review & editing: Wouters L, Caenen A, Youssef A, Araujo Andrade Sousa A, Bézy S, Duchenne J, D'Hooge J, Voigt JU.

of great clinical value. This review aims at introducing the fundamental physical and physiological concepts of myocardial stiffness, will discuss the echocardiographic techniques able to assess it (e.g., cardiac shear wave [SW] elastography, time-harmonic elastography and acoustic radiation force [ARF] impulse imaging), and will provide a comprehensive overview of initial experience from clinical studies. Given its more frequent application in clinical research, SW elastography will be discussed more elaborately than the other techniques.

WHAT IS (MYOCARDIAL) STIFFNESS?

In general, stiffness describes an object's resistance to deformation in response to an applied force. A simple example is pulling on a spring. The stiffer the spring, the more force is needed to cause a certain elongation. In physics, this is described by Hooke's law, in which the elastic (or Young's) modulus (E) relates stress (σ) (i.e., the amount of force per unit area) to strain (ε) (i.e., the amount of deformation per unit length).[8]

$$\sigma = E \cdot \varepsilon$$

A 3-dimensional (3D) object can deform in different ways, and there are different types of elastic moduli, depending on the type of deformation. In ultrasound elastography, we focus on the shear modulus, which relates shear stress to strain. Shear deformation causes a change in shape without a change in volume (**Figure 1**).

In the heart, stiffness can be evaluated on two levels. First, myocardial stiffness, defined as the local mechanical properties of the myocardium. It comprises both, passive material properties of the tissue and the active force development during contraction. The pure passive material properties determine myocardial stiffness from the end of relaxation until the beginning of the next contraction (end-diastole, mitral valve closure [MVC]). They form non-linear, upwards-curved stress-strain relation (**Figure 2A**).[1)9)10)] Chamber stiffness, on the other hand, describes the overall stiffness of a heart chamber as an entity. It depends on the stiffness of the myocardium that forms the chamber, but is modulated by chamber geometry,

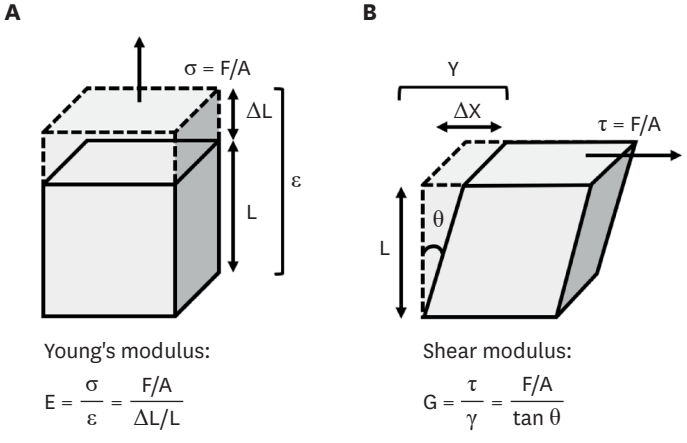

Figure 1. Examples of different types of elastic moduli: Young's modulus relates perpendicular stress to perpendicular strain (A), shear modulus relates tangential stress to shear strain (B). In a 3-dimensional object, deformation may be described by up to 81 different deformation tensors.[8]
A = area; ΔL = difference in length; E = Young's modulus; ε = strain; F = Force; G = shear modulus; γ = shear strain; L = length; σ = stress; τ = shear stress; tan θ = resulting shear of the material.

https://doi.org/10.4070/kcj.2025.0420

kcj
Korean Circulation Journal

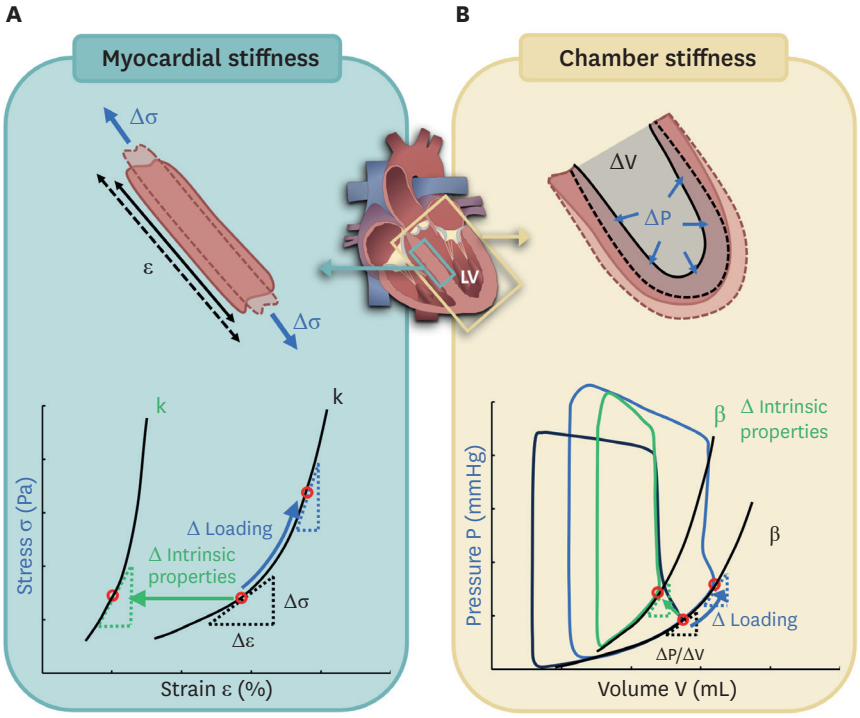

Figure 2. Myocardial stiffness and chamber stiffness. Myocardial stiffness (A) describes the relative elongation of the myocardial (strain, ε) wall in response to the wall stress (σ). This wall stress is caused by the filling pressure of the cavity but also modulated by the wall thickness and chamber size and shape. The end-diastolic stress-strain relation (black curves) is curvilinear and can be characterized as a whole by an exponential function with the stiffness constant k as dominant variable. The operational stiffness (red dot) represents the instantaneous stiffness (Δσ over Δε) at a certain preload (wall stress). An increase in preload causes a shift (blue arrow) towards a higher operating myocardial stiffness without changes of intrinsic myocardial properties (along the same stress-strain relation, same k). Changes in intrinsic myocardial properties because of pathologic processes (e.g., fibrosis or ischemic scar) change the entire stress strain relation towards a steeper curve (increased stiffness constant k). The operating myocardial stiffness increases, even at the same preload (green arrow). Chamber stiffness (B) is a result of myocardial stiffness, modulated by wall thickness and ventricular size and shape. It describes the increase in volume (ΔV) relative to the increase in cavity pressure (ΔP). The end-diastolic pressure-volume-relation can be approximated by an exponential function with stiffness constant ß as dominating variable and describes the chamber properties independent from preload as a whole. The operational stiffness (red dot) is the instantaneous stiffness (ΔP over ΔV) at a certain preload (filling pressure). Also here, both, an increase in preload as well as a higher myocardial stiffness constant will result in higher operating stiffness (adapted from Gaasch et al.[1]).
LV = left ventricle.

such as wall thickness, chamber volume, and shape.[1)11)] Passive chamber stiffness, i.e., when all parts of the chamber myocardium are relaxed, forms a similar non-linear, upwards-curved relation in a pressure-volume (PV) diagram (**Figure 2B**), commonly referred to as the end-diastolic PV relation (EDPVR). Stress-strain- and PV-loops can be constructed to describe local myocardial and chamber function, respectively, throughout the cardiac cycle. The loop area of a stress-strain loop reflects the external work per volume unit performed by the local myocardium. The loop area of the pressure volume loop reflects the external work performed by the entire ventricle.

Both the end-diastolic stress-strain relation and the EDPVR can be approximated with an exponential equation. In this equation, stiffness constant k (stress-strain) and ß (EDPVR) are the most relevant variables. These stiffness constants define the shape and steepness of the exponential function. Changes in the properties of the myocardium, such as the intracellular and extracellular components and their interaction (e.g., the cytoskeleton and the extracellular matrix), could result in a change in shape and steepness of the end-diastolic relations, and with this, in a change of k and ß.[9)]

https://doi.org/10.4070/kcj.2025.0420

While k and ß describe the shape of entire curve and with this the passive properties of wall and chamber independent from preload, a specific point on the curves describes the instantaneous stiffness at a given preload: operating stiffness. The curvilinear end-diastolic relations imply, that operating stiffness of myocardium and chamber is different at each point of the curve. In particular, it increases with increasing preload (higher strain or volume), as the point of operating stiffness moves to a steeper part of the curve.[1] Operating stiffness can be determined by the slope of the tangent to the stress-strain or EDPVR curve (**Figure 2**).

With this, measuring operational stiffness offers a dynamic evaluation of the instantaneous mechanical state of the heart, reflecting both, the passive myocardial properties of the myocardium and the current state of preload.

Myocardial stiffness during systole, on the other hand, is dominated by cross-bridge formation, and is therefore an indicator of contractility. As such, evaluating myocardial stiffness could provide direct insight into both the systolic and diastolic performance of the heart. This makes echocardiographic stiffness assessment a potentially valuable tool in the clinical setting.

DETERMINATION OF MYOCARDIAL STIFFNESS BASED ON SHEAR WAVES

Nowadays, non-invasive methods to assess myocardial stiffness based on the detection of SWs are emerging: cardiac SW elastography (SWE) and cardiac time harmonic elastography (THE).[3)5)] SWs are transverse waves, i.e., the particle motion is perpendicular to the propagation direction of the wave (**Figure 3**). Interestingly, the propagation speed (c) of SWs is dependent on the shear modulus (G) of the material (Equation 1).[8)13-15)]

$$c = \sqrt{\frac{G}{\rho}} \qquad (1)$$

In a homogenous, isotropic material, Young's modulus (E) has a simple relation with G (Equation 2):

$$E = 3 \cdot G \qquad (2)$$

As such, SW speed can be described in relation to Young's modulus (Equation 3):

$$c = \sqrt{\frac{E}{3\,\rho}} \qquad (3)$$

The imaging modality of choice is echocardiography as it combines flexibility, feasibility and high temporal resolution, but the use of cardiac magnetic resonance imaging (MRI) has also been explored.

https://doi.org/10.4070/kcj.2025.0420

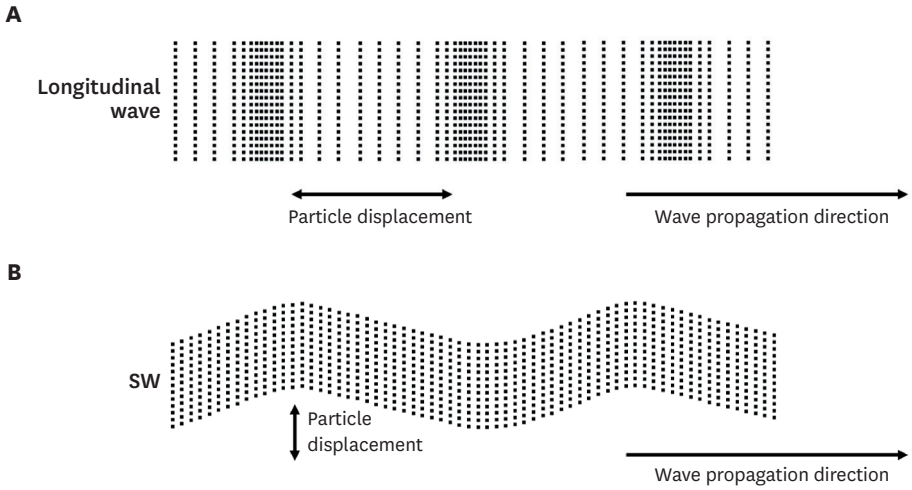

Figure 3. Example of a SW and a longitudinal wave. Schematic representation of a longitudinal wave of which the particle displacement is in line with the wave propagation (A) and a shear or transverse wave of which the particle displacement is perpendicular to the wave propagation (B).[12]
SW = shear wave.

Natural vs. induced shear waves

SWs in the myocardium are naturally generated by valve closure events. Such "natural SWs" occur, e.g.,, after aortic valve closure (AVC) and MVC and travel from the ventricular base to the apex (**Figure 4**).[13][14][16] Natural SWs are strong, easy to detect waves, but they are tied to specific events during the cardiac cycle and can therefore only provide information about myocardial stiffness at these particular time points.

SWs can also be "induced" using ARF (**Figure 4**).[16][17] In this technique, a strong focused ultrasound impulse is used to cause mechanical vibration of the tissue. With this, SWs can (in theory) be induced at any place in the myocardium at any point during the cardiac cycle, offering greater flexibility. However, ARF induced waves have lower amplitude, making them more difficult to be detected and less feasible to track over larger distances.

SWs can also be induced via an external vibrator. Mechanical longitudinal waves then travel through the body and cause SWs while they pass through the tissue. The latter can be observed using MRI or echocardiography (time harmonic imaging, THE) (**Figure 4**).[5] As vibrations have to travel across several layers of tissue (skin, ribcage, lungs, pericardium, etc.), low frequency vibrations are used, since they penetrate more easily in the body. However, such waves have a longer wavelength and are still considerably attenuated, which makes SW speed estimates more prone to errors. Furthermore, these waves also interact with all anatomical structures they encounter and movement of the heart can lead to inconsistencies in the force that external stimuli delivers to the myocardium, making its interpretation more difficult.[18]

Besides SWs, a mechanical wave following atrial contraction (atrial kick, AK) can be observed in the myocardium and has been explored for myocardial stiffness assessment. This mechanical stretching wave is most likely caused by a local pressure change in the ventricular cavity that originates from a blood vortex travelling to the apex after atrial contraction. Early studies have described this phenomenon using tissue Doppler under different loading conditions.[19] Other studies have investigated the AK wave speed in patients with aortic

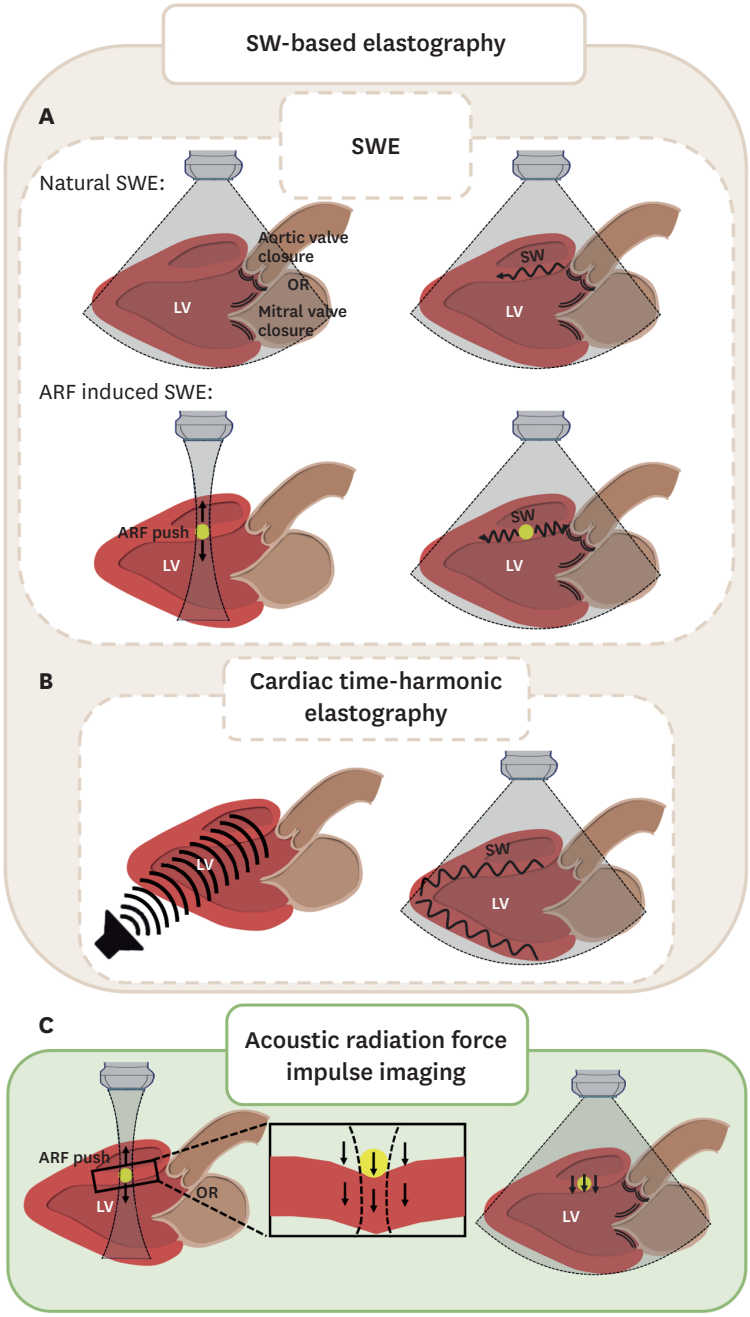

Figure 4. Overview of ultrasound-based techniques to determine myocardial stiffness. (A) SWE. The 2 most used techniques within SWE are shown: natural SWE, where SWs that arise from closure of the valves are tracked and ARF induced SWE, where SW are induced by sending a focused ultrasound push towards the septum. (B) Cardiac time-harmonic elastography. SWs are induced in the whole imaging window by sending low-frequency vibrations with an external vibrator. (C) Acoustic radiation force impulse imaging: This techniques looks directly at tissue displacement induced by an acoustic radiation force impulse to determine tissue stiffness. It is based on the principle that the magnitude of the ARF-displacement is inversely related to tissue stiffness.
ARF = acoustic radiation force; LV = left ventricle; SW = shear wave; SWE = shear wave elastography.

stenosis (AS),[20][21] cardiac amyloidosis (CA)[22] and hypertrophic cardiomyopathy (HCM) and in healthy volunteers (HVs).[23] However, the AK waves have different physical behavior than SWs and therefore, will not further be discussed in this paper.

https://doi.org/10.4070/kcj.2025.0420

Shear wave imaging

SWs travel along the myocardium with a relatively high propagation speed ranging from 1–10 m/s, requiring imaging with sufficient temporal resolution for their detection. Therefore, high frame rate (HFR) echocardiography is used for SWE based on natural or ARF-induced SWs.[13] In THE, where the frequency of the inducing waves is known, low frame rate stroboscopic sampling (controlled aliasing) is possible so that images can be acquired with regular echocardiography or even with (low frame rate) MRI.[5]

High frame rate echocardiography

In conventional 2D echocardiography, focused ultrasound pulses are emitted in different directions. Each pulse-echo event constructs one of approximately 180 image lines that form the 90° image sector. The acquisition of one line takes approximately 200 μs given a speed of sound in soft tissue of approximately 1,540 m/s and the round-trip distance between probe and the maximum image depth being typically 30 cm. Consequently, generating a complete image requires about 36 ms (180 lines × 200 μs), allowing for a frame rate of roughly 28 frames per second. Since both the speed of sound and the imaging depth are fixed, the only way to increase the frame rate is by reducing the number of pulses needed to form an image.[14] In modern ultrasound machines, images are constructed using multiline acquisition, in which the sent-out ultrasound beam is less focused and covers multiple scan lines that are then reconstructed in parallel (**Figure 5**). This can increase frame rate without significant loss in image quality to the 60 to 80 frames per second that are typical for contemporary echo machines.

HFR echocardiography uses diverging waves, that represent a single, unfocused ultrasound pulse that covers the entire image sector at once (**Figure 5**). This approach requires the live processing and intermediate storage of all signals received by all crystals of the probe to allow the subsequent reconstruction of all scan lines for one frame. Only recent developments in probe design and increases in computational power made the theoretical idea of diverging wave imaging (DWI), and with this SWE, become a reality. DWI dramatically increases the frame rate, theoretically up to 5,000 frames per second (1 frame per 200 μs), considering the same imaging depth of 15 cm. However, because the energy of each diverging wave pulse is spread across the entire image sector, the signal-to-noise ratio and the spatial resolution are reduced. To address this, coherent spatial compounding is applied, where subsequent acquisitions image the same region from slightly

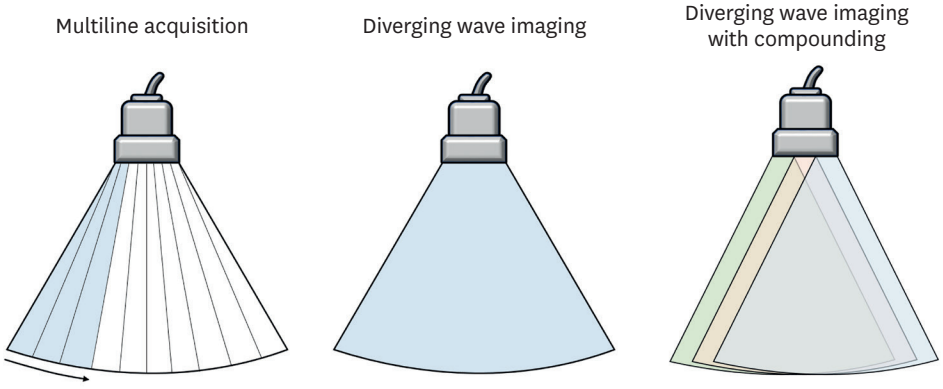

Figure 5. Schematic overview of different approaches to increase the temporal resolution of ultrasound imaging, such as multiline acquisition and diverging wave imaging with and without compounding.[12]

https://doi.org/10.4070/kcj.2025.0420

different angles and resulting images are combined (compounded) to form a single, higher-quality image. Depending on the number of compounded acquisitions, the effective frame rate is again reduced. For SWE, a frame rate of at least 1,000 frames per second should be maintained to appropriately image the propagating waves.[14]

Time-harmonic elastography: stroboscopic sampling

In THE, echocardiographic image acquisition is performed with a relatively low frame rate of around 100 frames per second. SWs are then imaged through 'controlled aliasing' or 'stroboscopic sampling' over several wave cycles. As the inducing wave frequency is known, the true signal can be recovered from the data.[5] A disadvantage of this approach is a longer acquisition time and sensitivity to myocardial motion. Any change during the acquisition due to noise or movement may cause distortion of the reconstructed wave. Furthermore, the wave propagation component in the desired direction (e.g., along the myocardial wall) needs to be reconstructed, causing additional error.

Wave speed assessment

Shear wave elastography

Compared to longitudinal waves, SWs are particularly advantageous for tissue characterization for several reasons. First, in soft tissue, their propagation speed spans over a wider range than in longitudinal waves, typically 1–10 m/s compared to 1,350–1,700 m/s, making it easier to detect variations in speed. Second, their speed increases significantly with pathological changes. Finally, simple Tissue Doppler processing can be used to track transverse SW propagation in the HFR images when the heart wall is imaged from the side.[24] The latter is the reason why SW speed is typically measured from a parasternal window. While natural SWs originating from the valves and travelling mainly from base to apex are best imaged in a parasternal long axis (PLAX) view, waves induced by ARF spread in all directions from the source of excitation and can therefore be investigated in both, PLAX and parasternal short axis views (SAX).[24,25] It is important to note that natural SWs are not 'pure' SWs. They also contain a longitudinal wave mode which can be imaged from the apical views. However, as the shear and longitudinal wave mode have different velocities and different response to myocardial changes, measured wave speeds, e.g., from a parasternal and an apical approach, cannot be interchangeably used.

To evaluate SW speed, an M-mode in the middle of the anteroseptal wall is drawn. The M-mode display is then color-coded for tissue velocity or acceleration, so that SWs appear as tilted color bands. The slope of these bands represents SW propagation speed (**Figure 6**). An example of how these tissue velocity and acceleration maps are calculated can be found in.[13]

The slope can be measured using manual or semi-automatic approaches. An example of a semi-automatic way to determine SW speed in an acceleration map is as follows: first, the wave of interest is indicated with a mouse click and then automatically roughly segmented, e.g., by using a certain threshold (e.g., 1 mm/s^2). Next, the algorithm searches for the peak accelerations within this segmented area. A linear regression is applied to the found acceleration peaks, the slope of which reflects the propagation speed of the wave. In this way, the algorithm takes both the peak accelerations and the shape of the wave into account when determining the SW slope (**Figure 7**).[26] In our experience, this approach delivers more robust results compared to other methods of slope detection, e.g., a Radon transform.[27]

https://doi.org/10.4070/kcj.2025.0420

kcj
Korean Circulation Journal

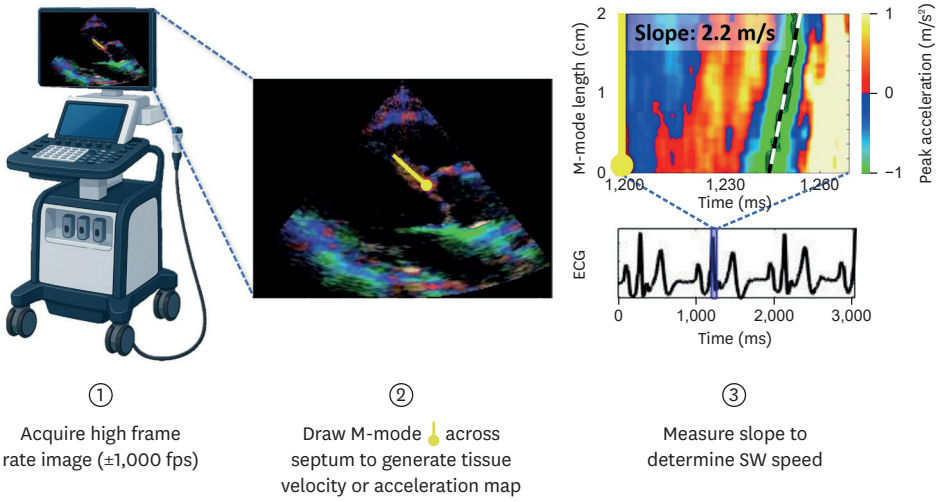

Figure 6. Technical steps to perform SWE. Three steps needed to perform SWE are 1) acquire a high frame rate image of around 1,000 frames per second. 2) post-processing of the images and an M-mode is drawn across the mid-septum from base to apex to generate a tissue velocity or acceleration map. 3) SWs are represented as tilted green bands in the velocity/acceleration maps. The slope of these bands are measured manually or semi-automatically to determine SW speed.
SW = shear wave; SWE = shear wave elastography.

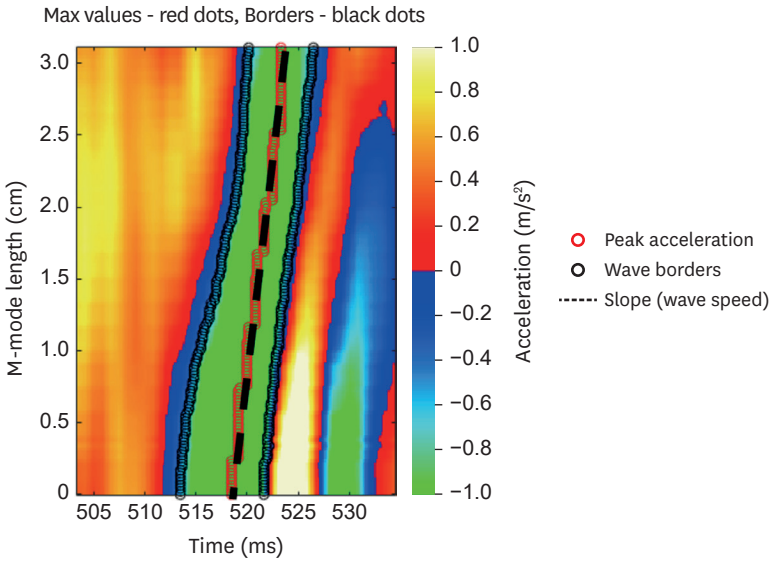

Figure 7. Measuring shear wave slope semi-automatically. The wave of interest is indicated with a mouse click and then segmented. The algorithm searches for the locations of the peak accelerations within the area and the borders of the segmented area. It then corrects the locations of the peak accelerations based on the edges of the segmented area. Finally, these corrected locations are used for a linear regression to determine the propagation speed of the wave.

Time-harmonic elastography

In THE, stiffness maps of the septal and posterior wall are created in the PLAX-view using a specific postprocessing algorithm (**Figure 8**). To generate these maps, the axial displacement of the tissue is tracked between each frame. Background noise from the overall movement of the heart (breathing, heartbeat, other movements) is reduced by applying a bandpass filter to isolate the frequencies of interest. As these waves travel through the tissue in all directions, directional filters are used to focus on the direction of interest. Finally, a stiffness map is

https://doi.org/10.4070/kcj.2025.0420

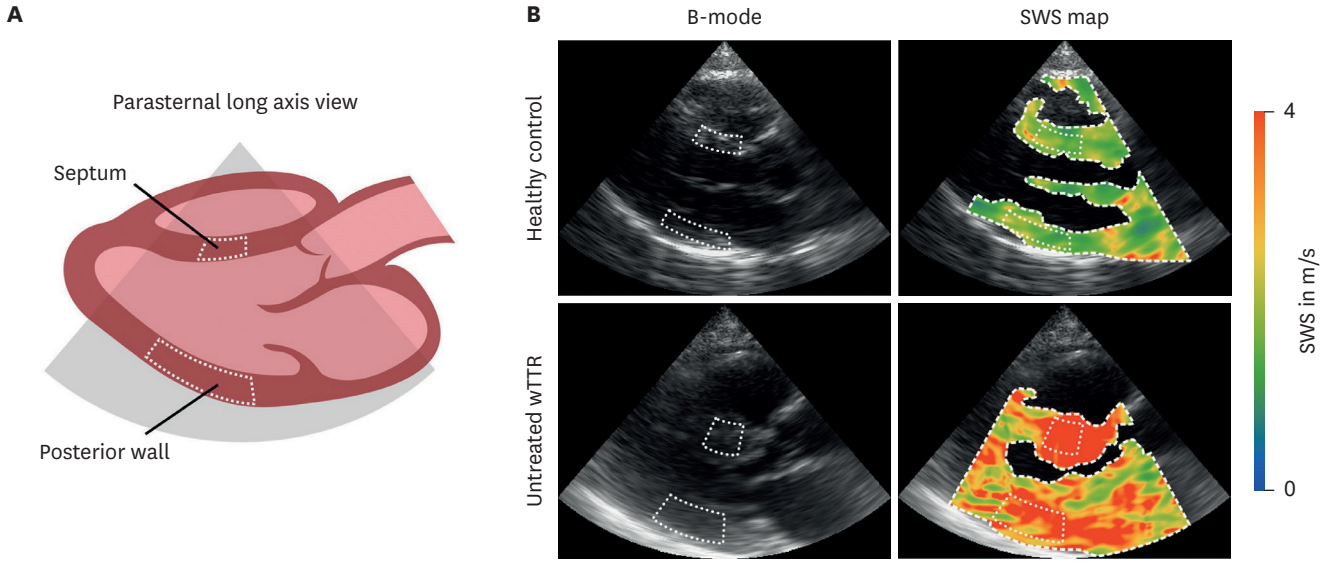

Figure 8. Example of cardiac time-harmonic elastography. (A) Anatomical overview of the measurements performed in the parasternal long-axis view. (B) Representative B-mode images and SWS maps of a healthy control subject and a hypertrophic cardiomyopathy patient. Regions of interest are demarcated by white dotted lines. Regions of interest of the septum and posterior wall were manually selected. A third region of interest (white dashed line in the SWS maps) was automatically identified to select a larger region of major portions of the myocardium visible in the image without any user interaction (adapted from Meyer et al.[5]). SWS = shear wave speed; wTTR = wild-type transthyretin amyloidosis.

constructed in which regions of interest can be defined for measuring stiffness in a certain area of the image.[5]

Factors that influence shear wave speed

SW speed is influenced by different factors that need to be considered when interpreting measurements (**Figure 9**).

Age: in HVs, myocardial stiffness derived from ARF-induced SW speeds in diastole has been shown to have a linear correlation with age (r=0.88 in HV of 20–80 years old and r=0.83 in HV of 0–45 years old) (**Figure 10**).[17][28] Likewise, there is also a clear relationship between age and natural SW speed after MVC in HV from 2–80 years old (r=0.71) (**Figure 9**).[29][30] This dependency could be explained by the changes in tissue properties with age due to accumulation of collagen and fibrotic remodeling of the myocardium. Interestingly, Youssef et al.[29] observed a strong non-linear correlation between SW speed and age in children from 2–10 years old, suggesting an impact of the rapid growth and changing geometry of the heart in young children.[29] These results advocate the use of age-specific reference values of SW speed. An overview of SW speed for every age category is given in **Table 1**.

The difference between the linear relationship of stiffness and the non-linear relationship of SW speed with age is explained by the conversion of SW speed to myocardial stiffness through a quadratic equation (see Equation 3). Furthermore, Malik et al.[28] and Villemain et al.[17] did not have many (or none) HV in the age group between 2–10 years old, where the largest increase in stiffness occurs. Finally, natural and induced SWs have different frequency spectra and may differ in their behavior.

Loading conditions: operational myocardial stiffness is dependent on tissue properties and loading. In preclinical animal experiments, changes in loading were achieved by saline infusion (preload increase) and caval/aortic balloon inflation (preload decrease/afterload

https://doi.org/10.4070/kcj.2025.0420

kcj
Korean Circulation Journal

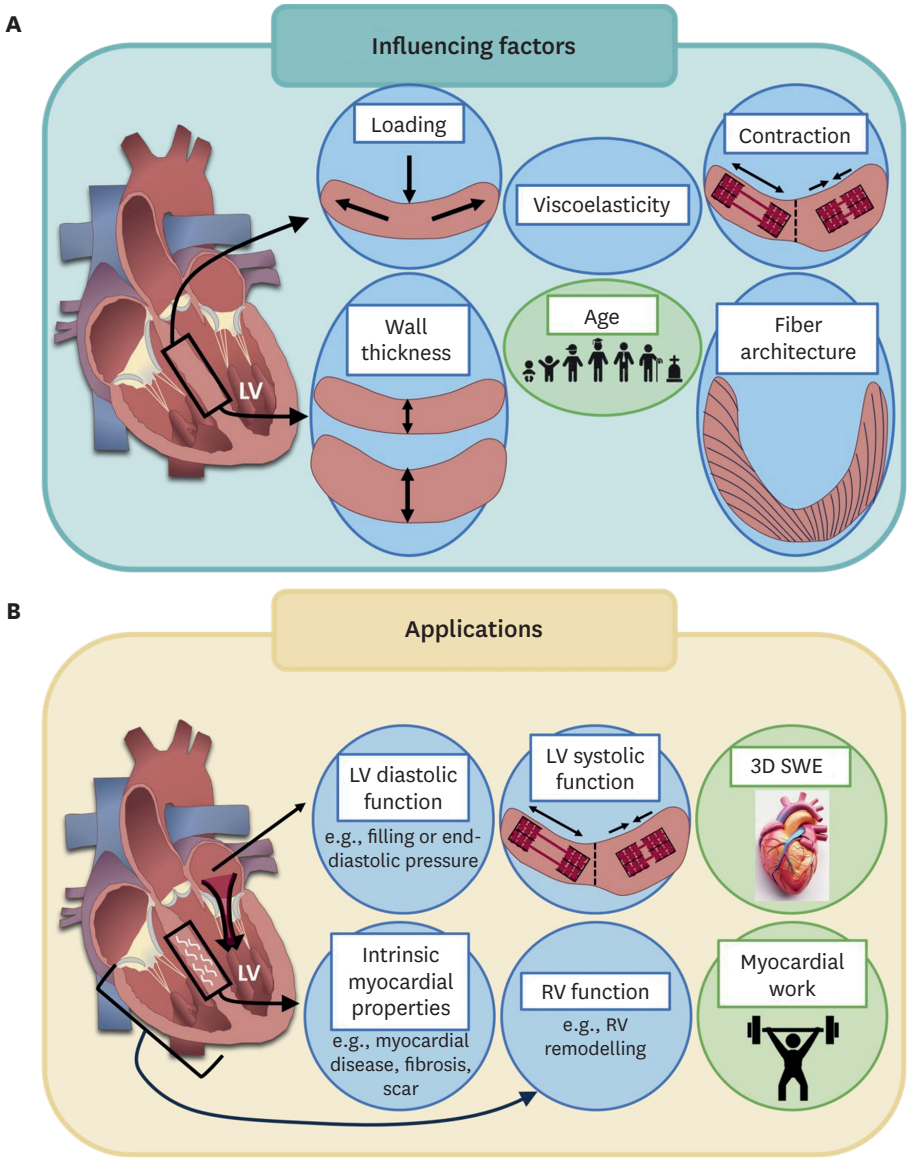

Figure 9. Influencing factors and applications. (A) shows factors that need to be considered when interpreting SW speed. Factors intrinsic to the heart are shown in blue, while factors related to demographics are shown in green. (B) shows the clinical applications of SWE: applications directly related to cardiac function are given in blue, while technical applications are shown in green.
LV = left ventricle; RV = right ventricle; SWE = shear wave elastography; 3D = three-dimensional.

increase) and SW speeds followed these changes (**Figure 11**).[7)18)31)32)] It should be noted that, preclinical studies using ARF-induced SWs found that diastolic SW speed was more closely related to intrinsic myocardial properties than to changes in loading conditions, although both had their influence.[7)31)] With natural SW speeds, the dependency on loading is stronger, e.g., a patient study using natural SW speed showed a correlation with invasively measured left ventricular (LV) diastolic pressures as well as pulmonary capillary wedge pressure (PCWP) (**Table 2**).[33)34)]

Timing: with ARF, SWs can be induced at any time during the cardiac cycle. For diastolic measurements, SW can be induced before atrial contraction or strictly at the end of diastole

https://doi.org/10.4070/kcj.2025.0420

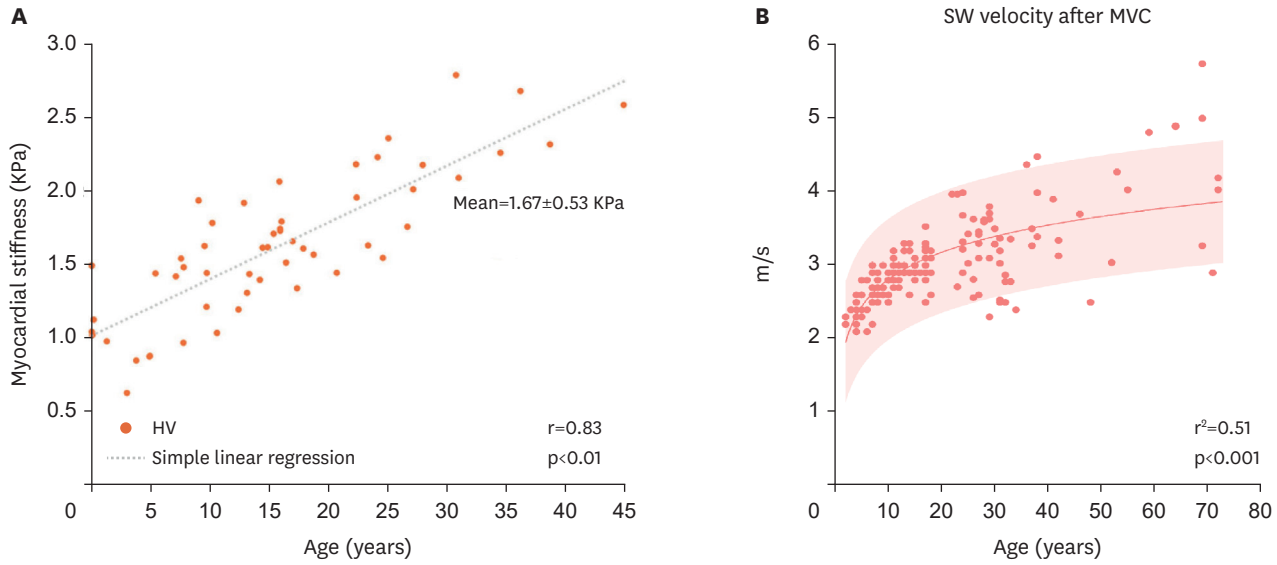

Figure 10. Correlations between myocardial stiffness or SW speed and age. (A) shows a linear correlation between myocardial stiffness (derived from acoustic radiation force-induced SW speed) in diastole and age in HVs (adapted from Malik et al.[28]). (B) shows the logarithmic relationship between natural SW speed after MVC and age in healthy volunteers.
HV = healthy volunteer; MVC = mitral valve closure; SW = shear wave.

Table 1. Overview of natural and ARF-induced SW speed across all age categories

Group	Age category	SW speed (m/s)	SW source	Reference
Children	<1 month	1.4±0.6	ARF (end-diastole)	Malik et al.[28]
	1 month–10 years	1.2±0.3		
	10–18 years	1.3±0.2		
	2–6 years	2.4±0.2	Natural SW (MVC)	Youssef et al.[29]
	7–12 years	2.7±0.2		
	13–18 years	3.0±0.2		
Adults	20–39 years	1.6±0.2	ARF (end-diastole)	Villemain et al.[17]
	40–59 years	2.2±0.2		
	60–80 years	4.3±0.6		
	20–39 years	3.1±0.5	Natural SW (MVC)	Petrescu et al.[30]
	40–59 years	3.8±0.8		
	60–80 years	4.5±1.1		
	20–39 years	3.5±0.7	Natural SW (AVC)	Petrescu et al.[30]
	40–59 years	3.8±0.8		
	60–80 years	4.3±0.6		

Values are presented as mean ± standard deviation.
ARF = acoustic radiation force; AVC = aortic valve closure; MVC = mitral valve closure; SW = shear wave.

and SW speed will then reflect the pure diastolic properties of the myocardium. In natural SWs on the other hand, speed is measured at the beginning of the isovolumic contraction phase, where rapidly changing pressures in the ventricle may already play a role. Studies so far, however, have shown a strong dependence of the speed of natural SWs after MVC on end-diastolic filling pressures and limited influence of contractility.[32][34] Left-bundle-branch-block-like conduction delays, however, that lead to a slow pressure rise in the chamber and a late MVC may lead to natural SWs after MVC that are—in part—influenced by the beginning contraction of the septum.[42]

Wall thickness: the simple relation between SW speed and myocardial stiffness as described by Equation 3 holds only true for homogeneous, isotropic bulk materials. In the heart however, SWs are reflected on the boundaries of the myocardium leading to wave guiding

https://doi.org/10.4070/kcj.2025.0420

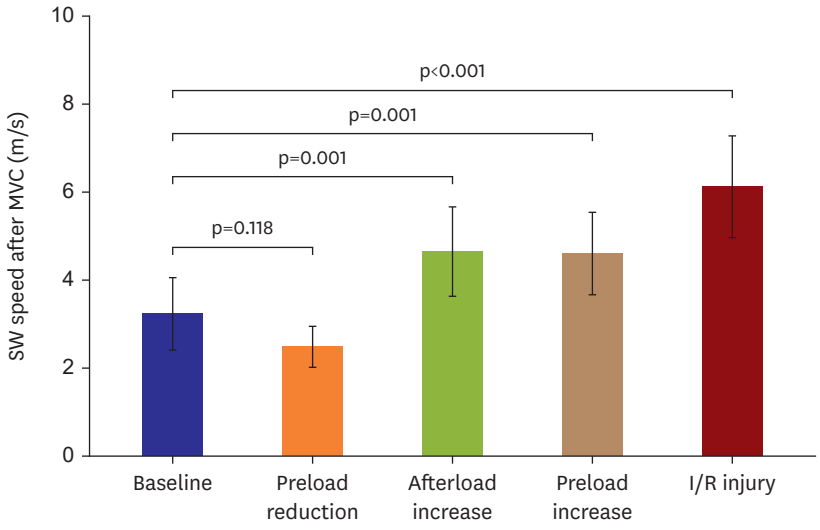

Figure 11. SW speed is influenced by loading conditions of the heart and changes in myocardial tissue properties.[32] I/R = ischemia-reperfusion; MVC = mitral valve closure; SW = shear wave.

Table 2. SW speed correlates with non-invasive and invasive markers of diastolic function

Type of diastolic parameter	Correlation with diastolic parameters	R-value	p value	AUC to detect increased filling pressures	SW source	Reference
Non-invasive	SW speed vs. e'	−0.409	0.001	Not mentioned	ARF (end-diastole)	Cafezeiro et al.[35]
	SW speed vs. E/e'	0.301	0.02	Not mentioned	ARF (end-diastole)	Cafezeiro et al.[35]
		0.61	<0.05	Not mentioned	Natural SW (AVC)	Jin et al.[36]
		0.74	0.002	Not mentioned	Natural SW (MVC)	Petrescu et al.[30]
		0.57	<0.001	Not mentioned	Natural SW (MVC)	Cvijic et al.[37]
		0.42	0.04	Not mentioned	Natural SW (AVC)	Strachinaru et al.[38]
		0.783	<0.01	Not mentioned	ARF (end-diastole)	Villemain et al.[17]
		0.54	<0.001	Not mentioned	Natural SW (MVC)	Popescu et al.[39]
		0.63	<0.01	Not mentioned	Natural SW (MVC)	Youssef et al.[29]
	SW speed vs. LAVI	0.324	0.012	Not mentioned	ARF (end-diastole)	Cafezeiro et al.[35]
	SW speed vs. diastolic function grade	0.361	0.009	Not mentioned	ARF (end-diastole)	Cafezeiro et al.[35]
Invasive	LV mid-diastolic pressure	0.65	<0.001	0.93	Natural SW (MVC)	Youssef et al.[40]
		0.47	<0.001	0.79	Natural SW (MVC)	Werner et al.[34]
	LV end-diastolic pressure	0.78	<0.001	0.96	Natural SW (MVC)	Youssef et al.[41]
		0.71	<0.001	0.95	Natural SW (MVC)	Werner et al.[34]
	Pulmonary capillary wedge pressure	0.54	<0.001	0.72	Natural SW (MVC)	Petrescu et al.[33]

ARF = acoustic radiation force; AUC = area under the curve; AVC = aortic valve closure; LAVI = left atrial volume index; LV = left ventricle; MVC = mitral valve closure; SW = shear wave.

effects and wave dispersion, a frequency dependent change in wave speed that may result in an underestimation of the actual myocardial stiffness. The effect occurs particularly in natural SWs (larger wavelength) and children (thinner walls). Several clinical studies have shown a link between wall thickness or LV mass index and SW speed.[28][29][36][37] Therefore, wall thickness should be reported or taken into account.

In THE, an even lower frequency wave is used to induce SWs causing also stronger guiding effects. However, as the frequency of the induced SW is known, it would in theory be possible to correct for this effect. However, this has not yet been tested in in vivo data.[43]

Contractility: cross-bridge formation and rising pressures in the LV increase myocardial stiffness during systole. Malik et al.[44] showed that ARF-induced SW speed increased during systole to a peak value of 3.8±0.7 m/s, while average SW speed during diastole was

https://doi.org/10.4070/kcj.2025.0420

1.6±0.2 m/s. ARF induced SWs therefore offer the option to investigate both, systolic and diastolic properties of the heart. Natural SWs may in part reflect contractility as they are always measured in an isovolumetric phase. While this effect appears small for natural SWs after MVC (end-diastole) it may be considerable for those after AVC which makes their interpretation complex. In a clinical study, Bezy et al.[45] found a positive correlation between SW speed after AVC and the end-systolic elastance (Ees, a marker of LV contractility), while Taha et al.[46] reported a significant increase in HV during stress echo, while there was no change in endurance athletes. In the same study, Taha et al.[46] found that SW speed after MVC significantly increased during exercise in both groups and Bézy et al.[32] reported an increase in SW speed after MVC in pigs after administration of dobutamine. However, the latter study could not prove a correlation between dP/dt max and change in SW speed.[32] On the other hand, a study in patients with invasively measured filling pressures showed a strong correlation of LV end-diastolic pressure (LVEDP) and SW speed measured after MVC was independent of the contractile state of the heart.[34] These interesting but—in part—contradicting findings show that the exact effect of contractility on the propagation speed of natural SWs is complex and needs further investigation.

Viscoelasticity: viscoelasticity of the myocardium causes SW dispersion and attenuation due to absorption of the mechanical wave energy, leading to a frequency-dependent wave speed. This effect has been studied in preclinical settings.[6][18][43][47][48] Clinical studies have not yet been performed. THE would theoretically allow a compensation since the frequency of the induced SW is known, however, this has not yet been tested in vivo.[43]

Fiber architecture: SW speed depends on myocardial fiber orientation as SWs propagate faster along fibers than across. This can be demonstrated by comparing induced SWs in the short axis and long-axis views.[17] Modelling shows that this effect is most pronounced in induced SWs due to a shorter length of the waves.[49] The dependency of SW speed on the fiber architecture has the potential to detect fiber disarray, which might hold a diagnostic value, but needs further investigation.[17][50] As the propagation direction of natural SWs is predetermined, and since in current clinical approaches of transthoracic measurements of ARF induced SWs, averaging measurements over the entire thickness of the myocardial wall are needed in order to increase signal-to-noise-ratio, fiber orientation cannot be distinguished and remains a theoretical concern.

Measurement method: ARF induced and natural SWs have different frequency spectra and differ in their behavior. Measurements from both methods cannot be directly compared as both, SW speeds and speed changes in pathology may differ.[24][44]

Recommendations for the clinical use of shear wave based elastography

Especially in vivo, it is often difficult to determine the exact effect of each of the above mentioned factors. Limited image quality, low signal to noise ratio or different techniques to visualize SWs (e.g., tissue doppler imaging[13] vs. clutter filter wave imaging [CFWI][21]) complicate the interpretation of the measured SW speeds further. Future research should thus aim at a better understanding of which effects can influence SW measurements in a clinically relevant way. **Table 3** provides an overview of each influencing factor and recommendations to adjust for them when using SW based elastography.

Standardizing both the imaging procedure and the post-processing algorithm enables direct comparison across different studies and improves clinical implementation. For example,

https://doi.org/10.4070/kcj.2025.0420

Table 3. Overview of influencing factors of SW speed and suggestions how to potentially account for them

Factor influencing SW speed	Author's recommendation to adjust for this factor
Age	Create age-specific reference values.
Loading	Perform an SW measurement during a loading change (e.g., passive leg raise).
Timing	Only compare SWs measured in the same phase of the cardiac cycle (e.g., at end-diastole or after MVC).
Wall thickness	Report wall thickness, consider potential underestimation of stiffness in walls under 1 cm thickness.
Contractility	For assessment of diastolic properties, measure SW speed at end-diastole.
Viscoelasticity	Perform a frequency analysis to report the main excited frequency of the wave.
Fiber architecture	Perform SWE in multiple echocardiographic views (PLAX and PSAX) and compare speeds.
ARF vs. natural	Report type and time of SW measurement. Do not compare measurements obtained at different time points of the cardiac cycle or with different methods.

ARF = acoustic radiation force; MVC = mitral valve closure; PLAX = parasternal long axis view; PSAX = parasternal short axis view; SW = shear wave; SWE = shear wave elastography.

consistently using the same echocardiographic view during follow-up within a study is crucial to ensure that the same cardiac wall is assessed and the same SW component is tracked. In addition, temporal resolution should be maximized, while maintaining acceptable spatial resolution, and an electrocardiogram should be recorded during acquisition to accurately determine wave timing.

During post-processing, it is important to use the same parameter for describing motion data (e.g.,, displacement, velocity, or acceleration) consistently. SW speed should be determined using a (semi-)automatic slope detection algorithm applied uniformly throughout the study. To minimize variability, averaging measurements over multiple cardiac beats and images is recommended. Finally, converting SW speed to stiffness using Equation 3 is not advised, as this relies on invalid material assumptions for the myocardium; therefore, SW speed should be reported directly.

Clinical applications of shear wave elastography

Over the past few years, the application of SWE has been studied in various pathologies, demonstrating the potential versatility of SWE in clinical echocardiography (**Figure 9**). An overview of these studies is given below.

Normal hearts

Considering that SWE should be able to detect increased myocardial stiffness, it is primarily important to determine normal reference values of a healthy population. Due to age-dependency of SW speed, reference values for HV should always be given for certain age categories. Values reported in the literature per age category and SW type (induced vs. natural) are given in **Table 1**.[17)28-30)]

Myocardial disease

SW propagation speed reflects the intrinsic properties of the myocardium. In this way, changes in the intrinsic properties, such as deposition of amyloid proteins, formation of interstitial fibrosis during maladaptive remodeling, edema due to inflammation, damage to the myocardium after chemo- or radiotherapy etc., could influence SW speed.[17)23)30)35-37)41)] One early in-human study was performed using ARF-induced SWs in HV and patients with sarcomeric HCM. They showed that myocardial stiffness was significantly increased in HCM patients compared to HV (4.47±1.68 vs. 12.68±2.91 kPa; $p<0.01$).[17)] Further, Petrescu et al.[30)] demonstrated clearly elevated natural SW speeds in amyloidosis patients compared to HV (6.33±1.63 vs. 3.54±0.93 m/s; $p<0.001$). SW speed in different cardiac pathologies is shown in **Table 4**. These results show that cardiac SWE can differentiate pathologic from

https://doi.org/10.4070/kcj.2025.0420

Table 4. SW speed in different cardiac pathologies

Pathology	SW speed (m/s) in pathology vs. HV	p value	AUC to detect pathology	Cut-off (m/s)	Discriminating factor	Average age of patients	SW source	SWE technique	Reference
Cardiac amyloidosis	6.3±1.6 vs. 3.5±0.9	<0.001	Not mentioned	NA	Not mentioned	68.0	Natural SW (MVC)	TDI	Petrescu et al.[30]
	5.6±1.1 vs. 3.8±0.8	<0.001	Not mentioned	NA	Not mentioned	68.0	Natural SW (AVC)	TDI	Petrescu et al.[30]
	1.5±0.2 vs. 1.3±0.1	0.03	0.69	NA	CA vs. HV	69±8.2	ARF (end-diastole)	TDI	Cafezeiro et al.[35]
	5.6±1.1 vs. 3.8±1.1	<0.001	0.88	4.6	CA vs. HV	72.7±6.2	Natural SW (AVC)	TDI	Jin et al.[36]
HCM	3.7±0.3 vs. 2.4±0.2	<0.01	0.993	NA	HCM vs. HV	57±17.5	ARF (end-diastole)	TDI	Villemain et al.[17]
	6.9±1.1 vs. 4.7±0.8	<0.0001	Not mentioned	NA	Not mentioned	48±13	Natural SW (MVC)	TDI	Strachinaru et al.[38]
	5.1±0.7 vs. 3.6±0.5	<0.0001	0.98	4.0	HCM vs. HV	48±13	Natural SW (AVC)	TDI	Strachinaru et al.[38]
Hypertension	5.8±1.2 vs. 4.0±1.0	<0.001	0.971	5	Concentric hypertrophy vs. HV	59±14	Natural SW (MVC)	TDI	Cvijic et al.[37]
Heart transplantation	5.7±2.3 (HV not mentioned)	NA	Not mentioned	NA	Not mentioned	54.1±17.8	Natural SW (MVC)	TDI	Petrescu et al.[33]
Aortic stenosis	3.4±1.4 vs. 2.1±0.7	0.007	Not mentioned	NA	Not mentioned	69±12	Natural SW (AVC)	CFWI	Espeland et al.[21]
Fabry disease	1.4±0.2 vs. 1.3±0.1	0.03	Not mentioned	NA	Not mentioned	49±14.2	ARF	TDI	Cafezeiro et al.[35]
Cancer survivors	3.9±0.6 vs. 3.2±0.3	<0.001	Not mentioned	NA	Not mentioned	20±3	Natural SW (MVC)	TDI	Youssef et al.[41]
Myocardial infarction	7.7±1.2 vs. 4.6±1.1	<0.001	0.92	7.1	Septal infarct vs. HV	73±6	Natural SW (MVC)	TDI	Wouters et al.[42]
	8.7±1.2 vs. 3.4±1.0	<0.001	0.92	8.1	Interstitial fibrosis vs. replacement fibrosis	54.4±15.2	Natural SW (MVC)	TDI	Petrescu et al.[51]
Interstitial fibrosis	6.5±1.1 vs. 3.4±1.0	<0.001	0.95	6	No fibrosis vs. fibrosis	56.7±16.2	Natural SW (MVC)	TDI	Petrescu et al.[51]
Patients with increased LVEDP	7.3±2.3 vs. 3.6±0.9	<0.001	0.95	4.8	Elevated LVEDP vs. normal LVEDP	70±10	Natural SW (MVC)	TDI	Werner et al.[34]

The ability of SW speed to distinguish between HV and different pathologies is given by the AUC.
ARF = acoustic radiation force; AUC = area under the curve; AVC = aortic valve closure; CA = cardiac amyloidosis; CFWI = clutter filter wave imaging; HCM = hypertrophic cardiomyopathy; HV = healthy volunteers; LVEDP = left ventricular end-diastolic pressure; MVC = mitral valve closure; NA = not applicable; SW = shear wave; SWE = shear wave elastography; TDI = tissue doppler imaging.

healthy myocardium, which makes it a potentially valuable clinical tool for diagnosis and follow-up of patients.

Fibrosis and scar

As SWE gives direct insight into the intrinsic properties of the myocardium, it could potentially be used to detect presence of diffuse or replacement fibrosis. Until now, the presence of fibrosis is mostly determined using cardiac MRI. T1 mapping or the assessment of the extracellular volume fraction (ECV) are typically used to assess diffuse fibrosis, while late gadolinium enhancement describes the extent of myocardial scar. The ability of SWE to determine the presence of diffuse or replacement fibrosis has been investigated in several studies.[17][21][33][42][51] Good correlations were observed between SW speed after MVC and T1 mapping values and ECV (**Table 5**). Petrescu et al.[51] found good correlations between native T1 mapping and SW speed in heart transplant patients and HCM patients (r=0.48; p<0.001). However, the correlation between SW speed and ECV was even better (r=0.70; p<0.001).[51] Also, Villemain et al.[17] observed a good correlation between ARF-induced SW speed and T1 mapping in HV and HCM patients (r=0.71; p<0.01) and ECV and SW speed (r=0.45; p=0.03). Only Espeland et al.[21] found a weak correlation between SW speed after AVC and T1 mapping and ECV fraction. This might suggest that natural SW speed after

https://doi.org/10.4070/kcj.2025.0420

Table 5. Correlation between SW speed and indices of intrinsic myocardial tissue properties

Correlation with intrinsic myocardial properties	R-value	p value	SW source	SWE technique	Reference
SW speed vs. native T1	0.35	0.11	Natural SW (AVC)	CFWI	Espeland et al.[21]
	0.75	<0.001	Natural SW (MVC)	TDI	Petrescu et al.[33]
	0.48	<0.001	Natural SW (MVC)	TDI	Petrescu et al.[51]
	0.711	<0.01	ARF (end-diastole)	TDI	Villemain et al.[17]
SW speed vs. ECV	0.70	<0.001	Natural SW (MVC)	TDI	Petrescu et al.[51]
	0.14	0.55	Natural SW (AVC)	CFWI	Espeland et al.[21]
	0.447	0.03	ARF (end-diastole)	TDI	Villemain et al.[17]

ARF = acoustic radiation force; AVC = aortic valve closure; CFWI = clutter filter wave imaging; ECV = extracellular volume fraction; MVC = mitral valve closure; SW = shear wave; SWE = shear wave elastography; TDI = tissue doppler imaging.

MVC is a better time point to explore the passive intrinsic properties of the myocardium then after AVC. Furthermore the differing methodology (CFWI) of the latter study to determine SW propagation speed may also have had an influence on the results.

Whether SWE could detect replacement fibrosis was investigated by Petrescu et al.[51] and Wouters et al.[42]. They both found that SW speed was increased in the presence of a septal scar (**Table 5**). Moreover, Wouters et al.[42] found that a cut-off of 7.1 m/s of SW speed after MVC could accurately detect the presence of a septal scar even in patients with a left bundle branch block. Petrescu et al.[51] found a cut-off value of 8.1 m/s for the best distinction of interstitial and replacement fibrosis (sensitivity and a specificity of 69 and 100%, area under the curve [AUC]=0.92) (**Figure 11**).

Loading conditions

Besides intrinsic properties, SW speed also reflects the filling status of the heart. As a result, it could be used to evaluate volume overload during acute cardiac decompensation and volume unloading after administration of diuretics. This was studied by Werner et al.,[34] who found a significant decrease in SW speed after MVC in patients with acute decompensation after administration of intravenous diuretics. Along the same line, Bezy et al.[52] investigated the effect of volume unloading on SW speed in patients undergoing hemodialysis. They found that SW speed significantly decreased 1 hour after the start of dialysis.[52]

Left ventricular diastolic function

Diastolic function is a complex interplay of active relaxation, chamber stiffness and early diastolic recoil leading to increased LV filling pressures as a common final pathway in most pathologies. In the clinic, the non-invasive assessment of diastolic function requires the interpretation of several echocardiographic parameters, which is complex, cumbersome and prone to errors. At end-diastole, SW speed reflects passive myocardial properties, which could make it an excellent tool to determine diastolic function. The correlation between SW speed and non-invasive (E/A, E/e', E-wave deceleration time) and invasive measures (LVEDP, PCWP) of diastolic function have been investigated in several studies (**Table 2**).[17,29,33-40] Overall, SW speed seems to be able to determine diastolic function, possibly even more precise than the conventional echocardiographic indices. In a study with 85 patients who underwent invasive measurements of filling pressures, Werner et al.[34] found that SWE could detect elevated LV mean-diastolic pressure as good as the currently used guideline algorithm (AUC of 0.79 vs. 0.78, not significant) while it outperformed the current guideline algorithm for the detection of elevated LVEDP (AUC of 0.95 vs. 0.60, p<0.001) (**Figure 12**). Therefore, using SW speed in addition to the conventional parameters could help to improve the

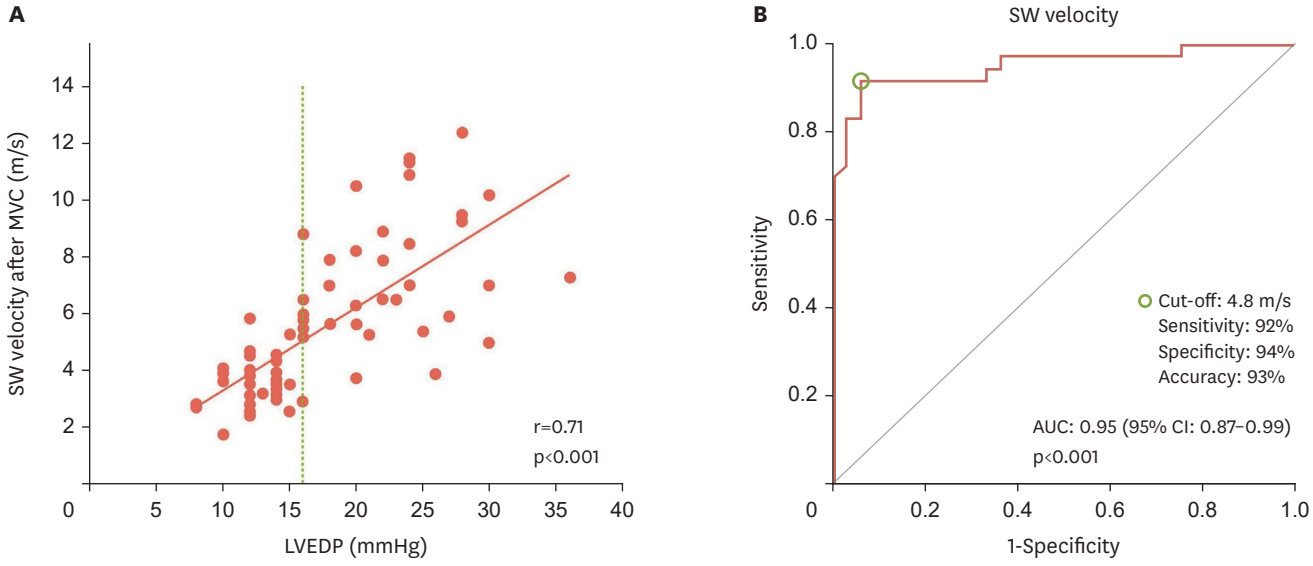

Figure 12. SW speed correlates with LVEDP and can accurately predict elevated filling pressures. (A) shows a correlation between SW speed and LVEDP. (B) shows the receiver operating characteristic analysis for SW speed to detect elevated LVEDP (adapted from Werner et al.[34]).
AUC = area under the curve; CI = confidence interval; LVEDP = left ventricular end-diastolic pressure; MVC = mitral valve closure; SW = shear wave.

diagnosis of diastolic dysfunction. Larger studies to confirm these early findings and to establish clinical cut-off values are currently performed.

In univentricular hearts, increased end-diastolic pressure is associated with a poor prognosis. However, determining diastolic dysfunction in these patients is difficult as conventional echocardiographic approaches are inadequate. Therefore, Salaets et al.[53] investigated whether SWE could determine diastolic stiffness in these patients. They showed that diastolic myocardial stiffness was significantly higher in the univentricular patient vs. HV.[53] This was also confirmed for natural SWs in other studies.[54][55] Own data using natural SWs, compared findings to invasively measured venous pressures in univentricular hearts. A correlation of r=0.55 (p=0.002) was observed.

Left ventricular systolic function

Myocardial contraction increases stiffness which is reflected by higher SW speeds during systole.[44] Potentially, ARF induced SWs at end-systole could therefore be used to determine end-diastolic elastance. Malik et al.[44] observed that there was no significant difference in SW speed between HCM patients and HV in mean systolic stiffness, in contrast to end-diastolic stiffness. This might indicate that systolic myocardial stiffness depends mostly on active myocardial properties (contractility), which is not different between HCM patients and controls.[44]

Right ventricular function

Most studies using SWE so far focused on the assessment of the LV function, but SW speeds both in the right ventricular (RV) free wall and in the septum may also be influenced by RV pathology. Venet et al.[27] investigated whether SWE could be used to determine RV remodeling pediatric patients with RV pressure overload. They measured natural SW speed after pulmonary valve closure (PVC) and tricuspid valve closure (TVC) in RV-focused parasternal and apical views. SW speed after TVC and after PVC was higher in patients with pressure overload compared to HV. Further, they showed a correlation between RV myocardial stiffness and hemodynamic parameters. This indicates that SWE is able to

https://doi.org/10.4070/kcj.2025.0420

determine myocardial stiffness in the RV, which suggests the potential utility of using SWE to track disease progression in the RV.

Nevertheless, SWE in the RV has technical challenges. The RV free wall is difficult to image and natural SWs after TVC or PVC are weaker and difficult to identify while SWs originating from MVC or AVC have a less well defined propagation direction on the RV.

Specific technical applications of shear wave elastography

Shear wave elastography in 3-dimensional

In SWE, a 2D image of the PLAX is used to track SW speed along the septum. However, SW propagation is a complex 3D phenomenon. Therefore, to properly understand SW speed propagation, 3D HFR echocardiography is needed. Papadacci et al.[56] investigated the propagation path of natural SWs using 4D ultrafast imaging. They found that natural SWs after AVC arise from a single source near the base of the heart that corresponds to the aortic valve position. The wave propagated along the anterior wall and the septum, consistent with the direction assessed in 2D. For the SW after MVC, 2 point-sources were identified which corresponded to the hinge regions of the 2 mitral valve leaflets. One source was located in the anteroseptal wall, which causes the SW observed in the PLAX view in 2D (**Figure 13**). Also, Caenen et al.[57] investigated the propagation of natural SWs, using the parasternal window to obtain a 3D data set. They found that for both the SWs after AVC and MVC, the wave propagation direction was from base to apex in the septum which justifies the assessment of SW speeds from a 2D PLAX view.[57] In both studies, measured SW speed was comparable in 2D and 3D for both valve closure events. It should be noted that both studies only included HV. Findings still need to be confirmed in pathologic hearts.

Shear wave elastography to determine myocardial work

Speckle tracking strain measurements have been proposed as basis for regional work assessment of the myocardium. Nevertheless, for the sake of clinical feasibility, such

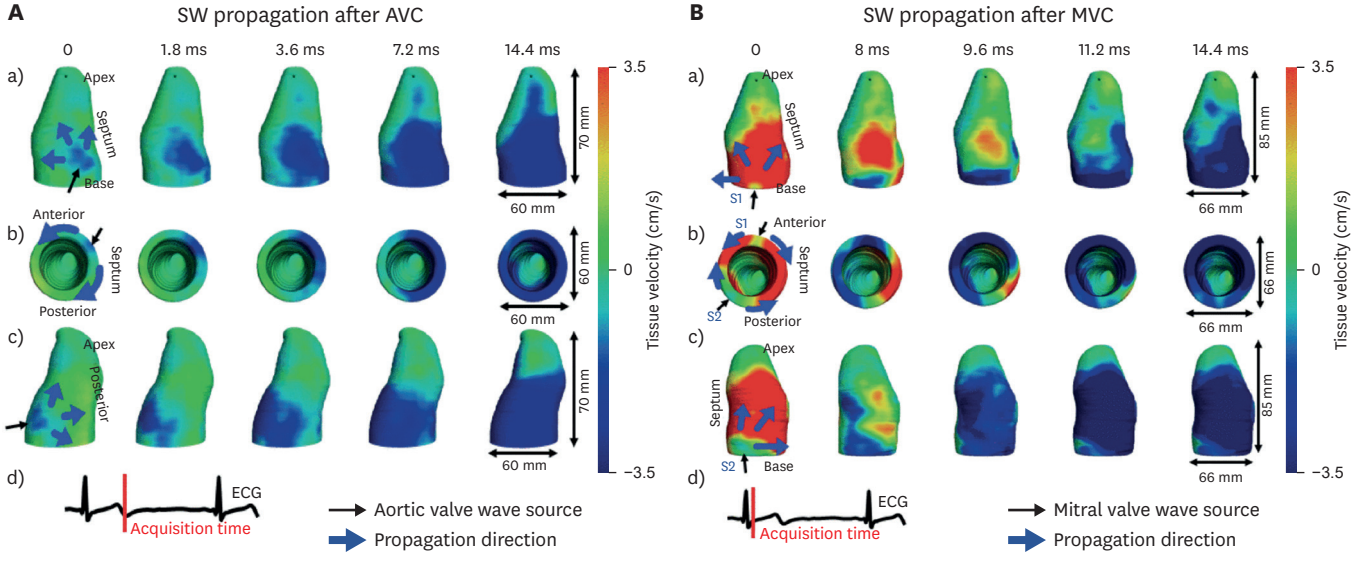

Figure 13. Representation of natural SW propagation after AVC (A) and MVC (B) across the LV in 3D. SW speed propagation after AVC originates from a point source at the anteroseptum, which corresponds to the aortic valve position. SW speed propagation after MVC seems to originate from 2 point sources, which correspond to the hinge points of the mitral valve leaflets. Overall wave propagation occurs from base to apex (adapted from Papadacci et al.[56]).
AVC = aortic valve closure; ECG = electrocardiogram; LV = left ventricle; MVC = mitral valve closure; SW = shear wave; 3D = three-dimensional.

https://doi.org/10.4070/kcj.2025.0420

approaches use estimates of the ventricular pressure for work calculations instead of invasively measured data. In theory, SWE would allow to calculate myocardial stress based on myocardial stiffness and deformation, and with this allow a completely non-invasive measurement of myocardial work. Venet et al.[58] have performed a proof-of-concept study in children with HCM, AS and HV. They induced SWs in the basal-anteroseptal wall at 20 different timepoints during the cardiac cycle to determine myocardial stiffness. Data were then used to calculate myocardial stress and eventually myocardial work. The authors report increased myocardial work in AS patients and a significant reduction in HCM. It should be noted, however, that the results were not directly compared to invasive gold standard measurements and that the presented stress-strain-loops did not resemble the shape that would be expected from invasive PV loops.[59] At the moment, the technique is limited to measuring myocardial work at the basal anteroseptal wall only.

Clinical applications of time-harmonic elastography

THE was performed by Meyer et al.[5] to quantify myocardial stiffness in patients with CA, HCM and HV in the septal and posterior wall. They showed that THE was feasible in all participants and that SW speed was higher in CA and HCM patients compared to HV (**Figure 8**). Furthermore, CA patients treated with Tafamidis had slightly lower SW speed values than untreated patients. Finally, THE could discriminate HV from CA and HCM patients based on SW speed with excellent and acceptable discriminative power respectively, showing that THE could become a promising tool to determine stiffness in different patient populations. However, further research is needed.[5]

Future of shear wave elastography

SWE could become a valuable tool to assess myocardial stiffness in a clinical setting. Many studies have confirmed the link between SW speed and echocardiographic or invasive measures of LV stiffness. SWE has also shown to be able to detect changes in intrinsic properties in various cardiac pathologies. However, further research is still needed. Large studies investigating direct comparisons between SW speed and closely related clinical parameters, such as invasive pressure measurements or MRI-based fibrosis assessment, are still missing and are essential before this promising tool can be used in clinical routine. For example, most studies were cross-sectional and conducted in a single center with a limited number of participants. Longitudinal studies could show the potential of SWE to help with patient management; while large multicenter studies are needed to confirm these findings. It should be noted that there is no non-invasive gold standard to determine cardiac stiffness in vivo, making a direct validation of SWE in clinical studies difficult. There is also a need for a more unified approach to acquire and analyze SW speed, to make the different findings of these studies more comparable. Overall, SWE remains a promising tool to non-invasively determine myocardial stiffness with a potentially significant role in daily patient management.

DETERMINATION OF MYOCARDIAL STIFFNESS BASED ON ACOUSTIC RADIATION FORCE IMPULSE IMAGING

Not only the propagation speed of SWs can be used as a measure of stiffness. Measuring how much an ARF impulse can move or deform tissue is a direct application of Hooke's law. In acoustic radiation force imaging (ARFI), myocardial stiffness is estimated from the tissue displacement at the location of the ultrasound push within the cardiac wall within a fixed time window after the force is applied (**Figure 4**).

https://doi.org/10.4070/kcj.2025.0420

ARFI can differentiate stiff from non-stiff tissue[60] and can be used to generate spatial or temporal maps of relative tissue stiffness.[61] By looking directly at displacement, ARFI is less susceptible to problems with the tracking of SWs due to attenuation or bias introduced due to changes in fiber orientation.[4] However, some challenges remain. First, the induced tissue displacement is small and difficult to distinguish from background noise. This becomes particularly challenging in stiffer hearts or in imaging at large depths. Further, the force applied through the ARF push is not defined, as the attenuation of the ultrasound impulse between probe and region of interest is not known. Measurement results are therefore dependent on the technical setup and the investigated individual and can be difficult to compare among studies or patients.

Clinical applications of acoustic radiation force impulse imaging

ARFI has already been tested in a clinical setting, although not as widely as SWE. Kakkad et al.[4] investigated the feasibility of ARFI in 12 HV in 2 echocardiographic views: PLAX and SAX. Overall, they found a median displacement of 3.04 μm in diastole, 1.19 μm in systole and 0.03 μm right before the push. ARFI was successful in 41% of the total acquisitions. This

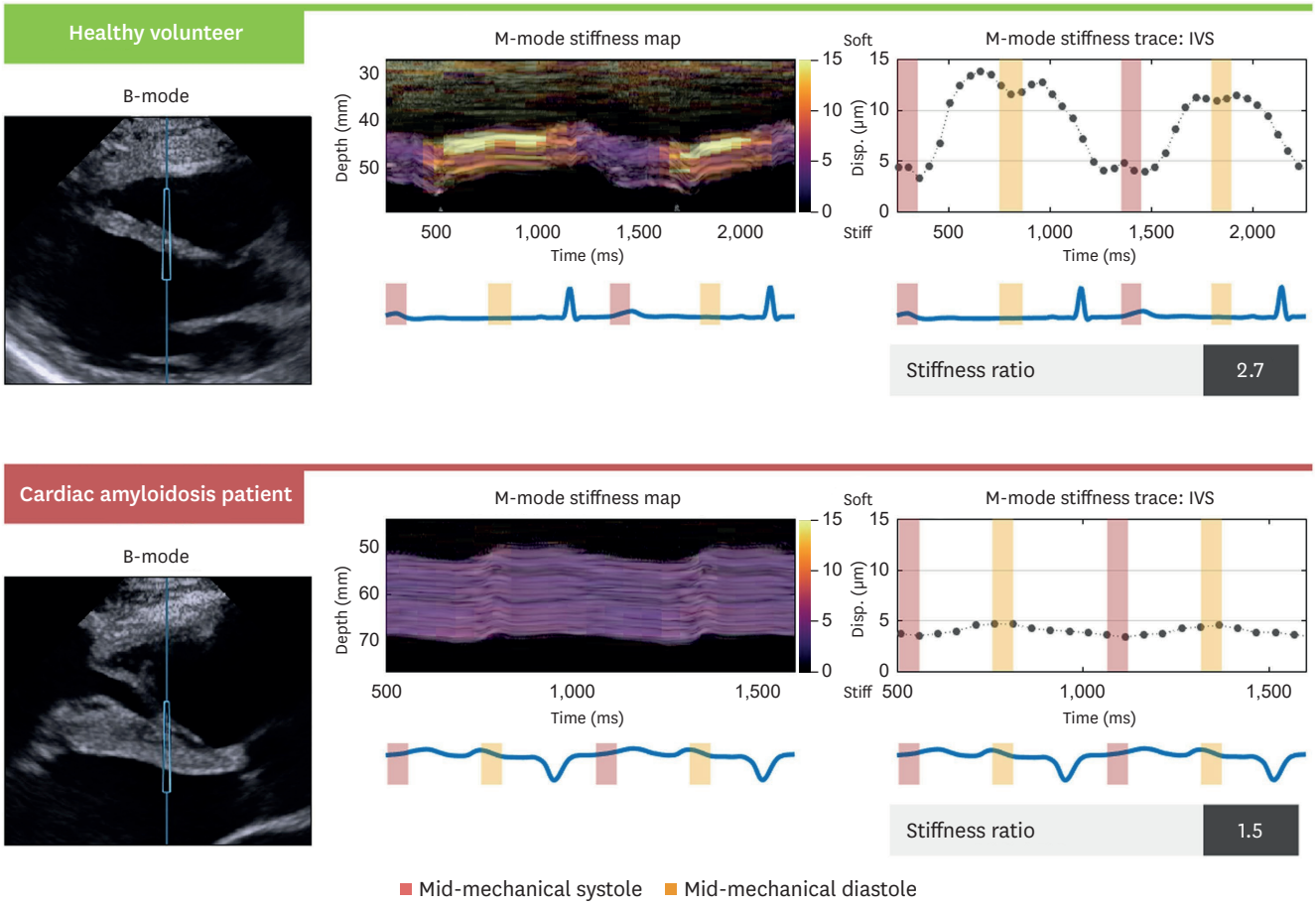

Figure 14. Example of ARFI data from a healthy volunteer and cardiac amyloidosis patient. On the left are B-mode images of the parasternal long-axis view of the IVS with the ARFI excitation and ROI marked by the vertical midline and blue box for an example healthy volunteer and a cardiac amyloidosis patient. In the middle, the M-modes from within the ROI box are shown with a color overlay of the ARFI displacement achieved 1.5 ms after each excitation. Mean ARFI displacement through the septum is shown in right plots, where yellow and red boxes indicate systolic and diastolic periods used for the stiffness ratio, the displacement measured in diastole over the displacement measured in systole. The electrocardiogram is shown beneath both the M-mode and mean displacement plots (adapted from Jin et al.[36]).
ARFI = acoustic radiation force impulse; IVS = interventricular septum; ROI = region of interest.

https://doi.org/10.4070/kcj.2025.0420

is a quite low success-rate, which could be attributed to the more challenging conditions of performing ARFI in transthoracic echocardiography.[4] ARFI was tested and compared to natural SW speeds in CA patients and HV by Jin et al.[36] They found that CA patients had lower peak diastolic displacements compared to HV (**Figure 14**). SW speed after AVC was also significantly higher in CA patients. These findings suggest an increased diastolic stiffness in CA patients.[36]

CONCLUSION

In this review we provided an overview of the newest echocardiographic-based methods to determine myocardial stiffness. Cardiac SW elastography is the most studied method in this field. Although SW speed is influenced by many different factors, making its interpretation rather complex, it shows great promise in assessing both systolic and diastolic function across various cardiac conditions and age groups, including in pediatric patients. Acoustic radiation force imaging and cardiac time-harmonic imaging may offer alternative approaches, but require further investigation. Given the importance of myocardial stiffness in many cardiac pathologies and the lack of easy-to-use, non-invasive tools to determine this parameter, SWE has the potential to play an important future role in patient diagnosis and management in daily clinical routine.

REFERENCES

1. Gaasch WH, Bing OHL, Mirsky I. Chamber compliance and myocardial stiffness in left ventricular hypertrophy. *Eur Heart J* 1982;3 Suppl A:139-45. PUBMED | CROSSREF
2. Granzier HL, Irving TC. Passive tension in cardiac muscle: contribution of collagen, titin, microtubules, and intermediate filaments. *Biophys J* 1995;68:1027-44. PUBMED | CROSSREF
3. Caenen A, Bézy S, Pernot M, et al. Ultrasound shear wave elastography in cardiology. *JACC Cardiovasc Imaging* 2024;17:314-29. PUBMED | CROSSREF
4. Kakkad V, LeFevre M, Hollender P, Kisslo J, Trahey GE. Non-invasive measurement of dynamic myocardial stiffness using acoustic radiation force impulse imaging. *Ultrasound Med Biol* 2019;45:1112-30. PUBMED | CROSSREF
5. Meyer T, Wellge B, Barzen G, et al. Cardiac elastography with external vibration for quantification of diastolic myocardial stiffness. *J Am Soc Echocardiogr* 2025;38:431-42. PUBMED | CROSSREF
6. Kanai H. Propagation of spontaneously actuated pulsive vibration in human heart wall and in vivo viscoelasticity estimation. *IEEE Trans Ultrason Ferroelectr Freq Control* 2005;52:1931-42. PUBMED | CROSSREF
7. Pernot M, Couade M, Mateo P, Crozatier B, Fischmeister R, Tanter M. Real-time assessment of myocardial contractility using shear wave imaging. *J Am Coll Cardiol* 2011;58:65-72. PUBMED | CROSSREF
8. Sigrist RMS, Liau J, Kaffas AE, Chammas MC, Willmann JK. Ultrasound elastography: review of techniques and clinical applications. *Theranostics* 2017;7:1303-29. PUBMED | CROSSREF
9. Villalobos Lizardi JC, Baranger J, Nguyen MB, et al. A guide for assessment of myocardial stiffness in health and disease. *Nat Cardiovasc Res* 2022;1:8-22. PUBMED | CROSSREF
10. Guimarães CF, Gasperini L, Marques AP, Reis RL. The stiffness of living tissues and its implications for tissue engineering. *Nat Rev Mater* 2020;5:351-70. CROSSREF
11. Burkhoff D, Mirsky I, Suga H. Assessment of systolic and diastolic ventricular properties via pressure-volume analysis: a guide for clinical, translational, and basic researchers. *Am J Physiol Heart Circ Physiol* 2005;289:H501-12. PUBMED | CROSSREF
12. Bézy S, Voigt JU, D'hooge J. Cardiac shear wave elastography for the assessment of myocardial stiffness [dissertation]. [Leuven]: KU Leuven; 2023.
13. Santos P, Petrescu AM, Pedrosa JP, et al. Natural shear wave imaging in the human heart: normal values, feasibility, and reproducibility. *IEEE Trans Ultrason Ferroelectr Freq Control* 2019;66:442-52. PUBMED | CROSSREF

14. Cikes M, Tong L, Sutherland GR, D'hooge J. Ultrafast cardiac ultrasound imaging: technical principles, applications, and clinical benefits. *JACC Cardiovasc Imaging* 2014;7:812-23. PUBMED | CROSSREF
15. Greenleaf JF, Fatemi M, Insana M. Selected methods for imaging elastic properties of biological tissues. *Annu Rev Biomed Eng* 2003;5:57-78. PUBMED | CROSSREF
16. Villemain O, Baranger J, Friedberg MK, et al. Ultrafast ultrasound imaging in pediatric and adult cardiology: techniques, applications, and perspectives. *JACC Cardiovasc Imaging* 2020;13:1771-91. PUBMED | CROSSREF
17. Villemain O, Correia M, Mousseaux E, et al. Myocardial stiffness evaluation using noninvasive shear wave imaging in healthy and hypertrophic cardiomyopathic adults. *JACC Cardiovasc Imaging* 2019;12:1135-45. PUBMED | CROSSREF
18. Pislaru C, Urban MW, Pislaru SV, Kinnick RR, Greenleaf JF. Viscoelastic properties of normal and infarcted myocardium measured by a multifrequency shear wave method: comparison with pressure-segment length method. *Ultrasound Med Biol* 2014;40:1785-95. PUBMED | CROSSREF
19. Voigt JU, Lindenmeier G, Werner D, et al. Strain rate imaging for the assessment of preload-dependent changes in regional left ventricular diastolic longitudinal function. *J Am Soc Echocardiogr* 2002;15:13-9. PUBMED | CROSSREF
20. Pislaru C, Alashry MM, Thaden JJ, Pellikka PA, Enriquez-Sarano M, Pislaru SV. Intrinsic wave propagation of myocardial stretch, a new tool to evaluate myocardial stiffness: a pilot study in patients with aortic stenosis and mitral regurgitation. *J Am Soc Echocardiogr* 2017;30:1070-80. PUBMED | CROSSREF
21. Espeland T, Wigen MS, Dalen H, et al. Mechanical wave velocities in left ventricular walls in healthy subjects and patients with aortic stenosis. *JACC Cardiovasc Imaging* 2024;17:111-24. PUBMED | CROSSREF
22. Pislaru C, Ionescu F, Alashry M, et al. Myocardial stiffness by intrinsic cardiac elastography in patients with amyloidosis: comparison with chamber stiffness and global longitudinal strain. *J Am Soc Echocardiogr* 2019;32:958-968.e4. PUBMED | CROSSREF
23. Strachinaru M, Geleijnse ML, de Jong N, et al. Myocardial stretch post-atrial contraction in healthy volunteers and hypertrophic cardiomyopathy patients. *Ultrasound Med Biol* 2019;45:1987-98. PUBMED | CROSSREF
24. Caenen A, Pernot M, Nightingale KR, et al. Assessing cardiac stiffness using ultrasound shear wave elastography. *Phys Med Biol* 2022;67:02TR01. PUBMED | CROSSREF
25. Keijzer LBH, Strachinaru M, Bowen DJ, et al. Parasternal versus apical view in cardiac natural mechanical wave speed measurements. *IEEE Trans Ultrason Ferroelectr Freq Control* 2020;67:1590-602. PUBMED | CROSSREF
26. Wouters L, Minten L, Orlowska M, et al. The impact of valve stenosis and replacement on wave characteristics in cardiac shear wave elastography. *IEEE Open J Ultrason Ferroelectr Freq Control* 2025;5:114-8. CROSSREF
27. Venet M, Malik A, Gold S, et al. Impact of right ventricular pressure overload on myocardial stiffness assessed by natural wave imaging. *JACC Cardiovasc Imaging* 2025;18:211-25. PUBMED | CROSSREF
28. Malik A, Baranger J, Nguyen MB, et al. Impact of ventricular geometric characteristics on myocardial stiffness assessment using shear-wave velocity in healthy children and young adults. *J Am Soc Echocardiogr* 2023;36:849-57. PUBMED | CROSSREF
29. Youssef AS, Petrescu A, Salaets T, et al. Evolution of natural myocardial shear wave behavior in young hearts: determinant factors and reproducibility analysis. *J Am Soc Echocardiogr* 2024;37:1051-61. PUBMED | CROSSREF
30. Petrescu A, Santos P, Orlowska M, et al. Velocities of naturally occurring myocardial shear waves increase with age and in cardiac amyloidosis. *JACC Cardiovasc Imaging* 2019;12:2389-98. PUBMED | CROSSREF
31. Caenen A, Keijzer L, Bézy S, et al. Continuous shear wave measurements for dynamic cardiac stiffness evaluation in pigs. *Sci Rep* 2023;13:17660. PUBMED | CROSSREF
32. Bézy S, Duchenne J, Orlowska M, et al. Impact of loading and myocardial mechanical properties on natural shear waves: comparison to pressure-volume loops. *JACC Cardiovasc Imaging* 2022;15:2023-34. PUBMED | CROSSREF
33. Petrescu A, Bézy S, Cvijic M, et al. Shear wave elastography using high-frame-rate imaging in the follow-up of heart transplantation recipients. *JACC Cardiovasc Imaging* 2020;13:2304-13. PUBMED | CROSSREF
34. Werner A, Bézy S, Wouters L, et al. Prediction of left ventricular filling pressures using natural shear waves: incremental value over conventional echocardiography. *JACC Cardiovasc Imaging* 2025;18:1071-89. PUBMED | CROSSREF
35. Cafezeiro CR, Neto AA, Romero CE, et al. Noninvasive assessment of myocardial stiffness using shear wave elastography in Amyloidosis and Fabry disease. *Curr Probl Cardiol* 2025;50:103038. PUBMED | CROSSREF

36. Jin FQ, Kakkad V, Bradway DP, et al. Evaluation of myocardial stiffness in cardiac amyloidosis using acoustic radiation force impulse and natural shear wave imaging. *Ultrasound Med Biol* 2023;49:1719-27. PUBMED | CROSSREF

37. Cvijic M, Bézy S, Petrescu A, et al. Interplay of cardiac remodelling and myocardial stiffness in hypertensive heart disease: a shear wave imaging study using high-frame rate echocardiography. *Eur Heart J Cardiovasc Imaging* 2020;21:664-72. PUBMED | CROSSREF

38. Strachinaru M, Bosch JG, van Gils L, et al. Naturally occurring shear waves in healthy volunteers and hypertrophic cardiomyopathy patients. *Ultrasound Med Biol* 2019;45:1977-86. PUBMED | CROSSREF

39. Popescu A, Cvijic M, Wouters L, et al. Ultrasound shear wave elastography for detection of myocardial fibrosis. *Eur Heart J Cardiovasc Imaging* 2025;26:jeae333.203. CROSSREF

40. Youssef A, Desmet W, Castaldi G, Frederiks P, Dhooge J, Voigt JU. Natural shear wave imaging outperforms conventional echocardiographic parameters in detecting elevated left ventricular filling pressures. *Eur Heart J Cardiovasc Imaging* 2025;26:jeae333.012. CROSSREF

41. Youssef A, Verschueren S, Vanrusselt D, et al. Early detection of cardiac dysfunction using shear wave imaging: insights into reduced cardiorespiratory fitness in childhood cancer survivors. *Eur Heart J* 2024;45:ehae666.148. CROSSREF

42. Wouters L, Duchenne J, Bézy S, et al. Septal scar detection in patients with left bundle branch block using echocardiographic shear wave elastography. *JACC Cardiovasc Imaging* 2023;16:713-5. PUBMED | CROSSREF

43. Nenadic IZ, Urban MW, Pislaru C, Escobar D, Vasconcelos L, Greenleaf JF. In vivo open- and closed-chest measurements of left-ventricular myocardial viscoelasticity using lamb wave dispersion ultrasound vibrometry (LDUV): a feasibility study. *Biomed Phys Eng Express* 2018;4:047001. PUBMED | CROSSREF

44. Malik A, Villalobos Lizardi JC, Baranger J, et al. Comparison between acoustic radiation force-induced and natural wave velocities for myocardial stiffness assessment in hypertrophic cardiomyopathy. *JACC Cardiovasc Imaging* 2024;17:223-5. PUBMED | CROSSREF

45. Bezy S, Cvijic M, Petrescu A, et al. Shear wave propagation velocity after aortic valve closure could be a novel parameter for myocardial contractility. *Eur Heart J Cardiovasc Imaging* 2020;21:jez319.034.

46. Taha K, Bekhuis Y, de Bosscher R, et al. Shear wave elastography to unmask differences in myocardial stiffness between athletes and sedentary non-athletes. *Eur Heart J Imaging Methods Pract* 2025;2:qyaf023. CROSSREF

47. Vos HJ, van Dalen BM, Heinonen I, et al. Cardiac shear wave velocity detection in the porcine heart. *Ultrasound Med Biol* 2017;43:753-64. PUBMED | CROSSREF

48. Urban MW, Pislaru C, Nenadic IZ, Kinnick RR, Greenleaf JF. Measurement of viscoelastic properties of in vivo swine myocardium using lamb wave dispersion ultrasound vibrometry (LDUV). *IEEE Trans Med Imaging* 2013;32:247-61. PUBMED | CROSSREF

49. Urban MW, Qiang B, Song P, Nenadic IZ, Chen S, Greenleaf JF. Investigation of the effects of myocardial anisotropy for shear wave elastography using impulsive force and harmonic vibration. *Phys Med Biol* 2016;61:365-82. PUBMED | CROSSREF

50. Lee WN, Pernot M, Couade M, et al. Mapping myocardial fiber orientation using echocardiography-based shear wave imaging. *IEEE Trans Med Imaging* 2012;31:554-62. PUBMED | CROSSREF

51. Petrescu A, Cvijic M, Wouters L, et al. Ultrasound shear wave elastography for detection of myocardial fibrosis. *Eur Heart J Cardiovasc Imaging* 2025;26:1537-45. CROSSREF

52. Bezy S, Orlowska M, Van Craenenbroeck A, et al. The change in propagation speed of natural shear waves by altering preload might differentiate patients with increased myocardial stiffness. *Eur Heart J Cardiovasc Imaging* 2023;24:jead119.242. CROSSREF

53. Salaets T, Venet M, Malik A, Baranger J, Mertens L, Villemain O. Diastolic myocardial stiffness assessed by shear wave elastography in children with a fontan circulation. *J Am Soc Echocardiogr* 2024;37:1116-8. PUBMED | CROSSREF

54. Cattapan I, Youssef A, Caenen A, et al. Natural shear wave elastography to assess diastolic function in univentricular hearts: a prospective cohort study. *Eur Heart J Cardiovasc Imaging* 2023;24:jead119.214. CROSSREF

55. Youssef A, Van Belle H, Dhooge J, Voigt JU, Van De Bruaene A. Increased myocardial stiffness as assessed by echocardiographic shear wave imaging is associated with Fontan circulatory failure. *Eur Heart J Cardiovasc Imaging* 2025;26:jeae333.212. CROSSREF

56. Papadacci C, Finel V, Villemain O, Tanter M, Pernot M. 4D ultrafast ultrasound imaging of naturally occurring shear waves in the human heart. *IEEE Trans Med Imaging* 2020;39:4436-44. PUBMED | CROSSREF

57. Caenen A, Papangelopoulou K, Wouters L, Seliverstova E, Voigt JU, D'Hooge J. 3D high-frame-rate imaging of natural shear waves in the parasternal view of the heart. *IEEE Open J Ultrason Ferroelectr Freq Control* 2025;5:1-5. CROSSREF

58. Venet M, Baranger J, Malik A, et al. Towards non-invasive assessment of myocardial work using myocardial stiffness and strain: a human pilot study. *Eur Heart J Cardiovasc Imaging* 2025;26:1051-64. PUBMED | CROSSREF

59. Voigt JU. Measuring the unmeasurable. *Eur Heart J Cardiovasc Imaging* 2025;26:1589-90. CROSSREF

60. Nightingale K, Soo MS, Nightingale R, Trahey G. Acoustic radiation force impulse imaging: in vivo demonstration of clinical feasibility. *Ultrasound Med Biol* 2002;28:227-35. PUBMED | CROSSREF

61. Palmeri ML, McAleavey SA, Fong KL, Trahey GE, Nightingale KR. Dynamic mechanical response of elastic spherical inclusions to impulsive acoustic radiation force excitation. *IEEE Trans Ultrason Ferroelectr Freq Control* 2006;53:2065-79. PUBMED | CROSSREF